(revised 4 September 96; Ninth International Conference on Fracture; Sydney; April 1997)

FATIGUE LIFE ASSESSMENT OF STEEL PRESSURE VESSELS WITH VARYING STRESS CONCENTRATION, RESIDUAL STRESS AND INITIAL CRACKS

J. H. UNDERWOOD

Army Armament Research, Development and Engineering Center
Watervliet, NY 12189 USA

A. P. PARKER

Visiting Professor, Royal Military College of Science, Cranfield University
Swindon SN6 8LA UK

ABSTRACT

A single parameter representation of local stress range, initial crack size and material yield strength is proposed for describing the intensity of the fatigue loading of a structural component. A logarithmic plot of single parameter fatigue life results provides a single straight line description of fatigue life behavior over a broad range of material, configuration and loading conditions. Expressions for calculating the local stress range at the failure site are outlined, including effects of vessel and stress concentrator configuration, applied and overstrain residual stresses, and pressure applied to hole and crack surfaces.

The single parameter approach was used in a comparison of fatigue life results from 41 full size cyclic hydraulic pressure tests of cannon pressure vessels with twelve combinations of material strength, failure location, and applied and residual stresses. A log plot of mean results of the twelve data groups is well represented by a single straight line with a negative slope reasonably close to that predicted by fracture mechanics analysis. A significant outlier from the straight line trend of the data is a useful indicator of cracking due to other than conventional mechanical fatigue. Two examples of an outlier from the trend of cannon pressure vessel data were confirmed by metallography to be caused by environmental cracking. A third outlier was related to preexisting initial cracks due to aggressive machining.

The effect of material yield strength on fatigue behavior can be simply and well represented using the single parameter approach. The correlation of a logarithmic straight line fit to the twelve sets of cannon pressure vessel results increased noticeably when the effect of material strength was included in the single parameter representation.

KEYWORDS

Metal fatigue, pressure vessels, fracture mechanics, high strength steels, residual stress, fatigue crack growth, stress concentration, stress - life curves

INTRODUCTION

The extensive testing of large caliber high strength steel cannon pressure vessels by Davidson *et al* (1977) provides a baseline of fatigue lifetime information that would be difficult to match today. This work included significant variation in residual stresses and material strength and some known differences in initial crack size at the vessel inner radius, all of which have important effects on fatigue life. The experimental life results were assessed in terms of fracture mechanics, with emphasis on the range of stress intensity factor, ΔK, and fatigue life calculations as a function of ΔK. In the past two decades, additional life testing of cannon pressure vessels has been performed, with emphasis on fatigue failures that occur away from the vessel inner radius at various types of stress concentration. Analysis to understand and describe these types of fatigue failure has been actively pursued.

Audino (1993) described a series of hydraulic pressure fatigue life tests in overstrained cannon tubes with failure locations both at the inner radius and at a notch in the outer radius. Underwood and Parker (1995) compared life results from overstrained cannon tubes containing erosion grooves at the inner radius with calculations using fracture mechanics. Underwood and coworkers (1995) analyzed several series of fatigue life tests of cannon tubes with various types of through-wall holes and different amounts of overstrain. Parker and coworkers (1996) performed fracture mechanics and fatigue life analyses for overstrained cannon tubes with axially oriented holes and compared the analytical predictions with life tests.

Recent work by Parker and Underwood (1997) has proposed a simple new method for representing fatigue life results by accounting for two fundamentally important control variables for fatigue life - local stress range and initial crack size - in a single parameter. Available methods for fatigue life assessment are often very complex or they do not include both of these control variables. The objective of the work here is to use this single parameter approach to describe the aforementioned fatigue lifetime results and thereby demonstrate its advantages and limitations in fatigue life analysis. The single parameter approach will be briefly summarized and then used to describe the cannon pressure vessel results in a derivative of the conventional stress range versus life presentation. By including all the appropriate applied and residual stresses and the stress concentration in an expression for the local stress range, and by adding initial crack size and material strength information, the new single parameter approach to fatigue life assessment is obtained. Critical comparisons of this single parameter approach with the large body of cannon pressure vessel lifetime results should show whether or not the approach has broad utility in representing fatigue life of pressure vessels.

ANALYSIS

The general types of fatigue cracking of cannon pressure vessels considered here are shown schematically in Figure 1, along with some of the nomenclature. The single parameter fatigue life analysis (Parker and Underwood, 1997) used to assess fatigue life for these various configurations is summarized, followed by the description of expressions for the local stress range at the site of fatigue cracking.

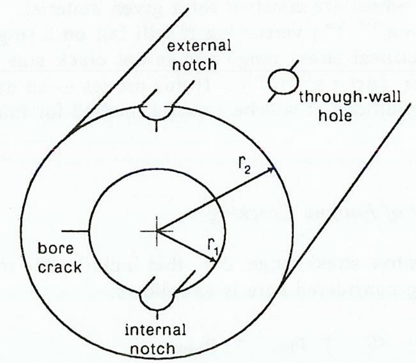

Fig. 1 - Some Types of Fatigue Cracking with Pressure Vessels

Single Parameter Fatigue Life Analysis

The Paris (1963) law describes a significant portion of the fatigue crack growth behavior, da/dN, of most metals:

$$da/dN = C\,(\Delta K)^m \tag{1}$$

where ΔK is the positive range of stress intensity factor and C and m are experimental constants. For steels m is often about 3 (Parker and Underwood, 1997). A general expression for ΔK is:

$$\Delta K = \Delta\sigma\,(\pi a)^{1/2} \tag{2}$$

where Δσ includes the constant, often near 1, relating to crack configuration and size. Combining Eq. (1) and (2) and integrating over the range from the initial crack size, a_i, to the critical crack size, a_c, gives:

$$N = [1/(C\,\pi^{m/2}\,\{1-m/2\}\{\Delta\sigma\}^m)]\,[\,a_c^{(1-m/2)} - a_i^{(1-m/2)}] \tag{3}$$

which is the basis of the work by Maddox (1971) relating the Paris law to the conventional log Δσ versus log N fatigue life presentation. Recognizing that the second term is constant for a given a_i and that typically $a_c >> a_i$, and taking logs leads to:

$$\log(\Delta\sigma) = (-1/m)\log N + (1/m - 1/2)\log a_i - (1/m)\log\{(m/2-1)\,C\,\pi^{m/2}\} \tag{4}$$

Finally, rearranging Eq. (4) leads to:

$$\log(\Delta\sigma \times a_i^{(1/2-1/m)}) = (-1/m)\log N - (1/m)\log\{(m/2-1)\,C\,\pi^{m/2}\} \tag{5}$$

which can be recognized as a straight line on log coordinates with slope (-1/m) and intercept

- (1/m) log {(m/2 -1) C $\pi^{m/2}$} which are constant for a given material. The form of Eq. (5) suggests that plots of log ($\Delta\sigma \times a_i^{(1/2 - 1/m)}$) versus log N will fall on a single straight line with (-1/m) slope and that all the critical stress range and initial crack size information will be included in the single parameter ($\Delta\sigma \times a_i^{(1/2 - 1/m)}$). If this proves to be true over a significant range of fatigue lifetime test conditions, it will be a useful method for fatigue life assessment.

Local Stress Range for Control of Fatigue Cracking

An expression for the local positive stress range, $\Delta\sigma$, that includes the important stresses for all the types of fatigue cracking considered here is as follows:

$$\Delta\sigma = k_{t\text{-}\theta}\,\sigma_\theta + k_{t\text{-}ov}\,\sigma_{ov} - \sigma_r + p_{hole} + p_{crack} \qquad (6)$$

The first two terms represent the stresses that often have the primary control of fatigue cracking in a pressure vessel, the applied and residual (due to overstrain) hoop direction stresses at the crack initiation site, σ_θ and σ_{ov}, sometimes multiplied by stress concentration factors, $k_{t\text{-}\theta}$ and $k_{t\text{-}ov}$, if a stress raiser is present. The third term accounts for the indirect effect of the compressive radial direction stress, σ_r, that, in a few cases here with a notch present, effectively adds to the tensile hoop stress at certain locations around the notch. For example at the crack locations in the internal and external notch radii shown in Fig. 1, the tensile hoop stress is increased by the (negative) value of the compressive radial stress at these locations. Near the vessel inner radius this effect of radial stress effectively adding to the hoop stress is significant. The last two terms in Eq. 6 account for the additional effect of pressure in the hole or in the crack. Pressure in a hole produces a tensile hoop stress at the hole inner radius with magnitude of about the value of pressure applied to the vessel. Pressure in the crack produces the equivalent of a tensile stress oriented normal to the crack plane that is also equal in magnitude to the applied pressure. So these two additional pressure effects, which add to the stresses in the vessel wall, can have significant control over fatigue life.

The expression used to calculate stress concentration factor at a notch is as follows, from Roark and Young (1975):

$$k_t = 1 + 2c/b \qquad (7)$$

where c is the depth of a semielliptically shaped notch and b is the half-width of the notch.

The local positive stress range at the site of fatigue cracking is calculated by elastic superposition of the terms in Eqs. (6) and (7) and is used in the single parameter presentation of fatigue life results as discussed in relation to Eq. (5), that is, a plot of $\Delta\sigma \times a_i^{(1/2 - 1/m)}$ versus N. These results are presented in the following section, with emphasis on the effects of overstrain residual stress, initial crack size, stress concentration, and material yield strength on the single parameter representation of fatigue lifetime.

RESULTS

Fatigue Failure at the Vessel Bore

A conventional $\Delta\sigma$ versus N plot of results from 24 cannon pressure vessel fatigue life tests is shown in Fig. 2 for fired (500 cannon firings typical before hydraulic pressure cycling) and

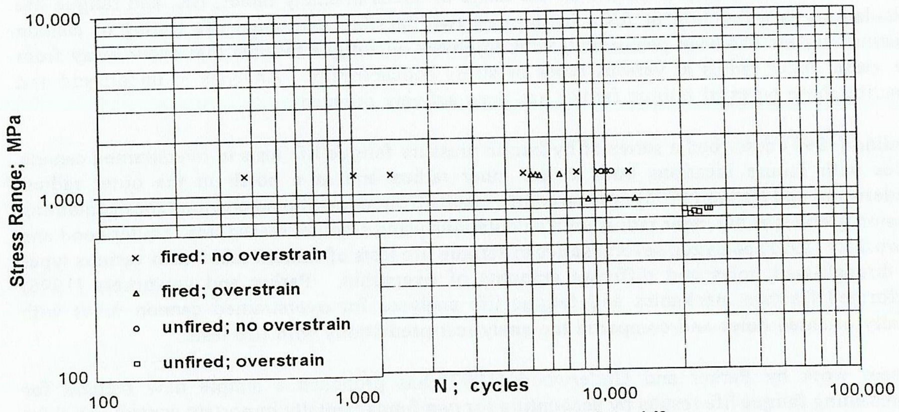

Fig. 2 - Effect of Bore Stress Range on Cannon Fatigue Life

unfired cannon tubes with and without a 50% overstrain residual stress. Table 1 lists key information from the tests, including the mean life for each of six types of vessel. Hydraulic oil pressure cycles were applied to 1 m long sections of cannon barrels at a load ratio of 0.1 and a frequency of 0.1 Hz. The failure location for these 24 tests was at the 0.5 mm root radius of one of the 1.8 mm high rifling lands at the bore of the cannon tube. The stress

Table 1 - Vessels with Fatigue Failure at the Bore; see Figs. 2 and 3

Type/Number of Vessels	Yield Strength *MPa*	Inner Radius *mm*	Outer Radius *mm*	Applied Pressure *MPa*	Stress Range *MPa*	Fatigue Life *cycles*	Initial Crack *mm*
FIRED; NO OVERSTRAIN							
a 3	1200	89	187	345	1275	10,039	0.1
b 4	1270	89	187	345	1275	4,110	0.5
1	1180	89	187	345	1275	373	> 0.5
FIRED; OVERSTRAIN							
c 4	1120	79	155	670	1247	5,590	0.1
d 3	1230	89	142	393	896	10,629	0.1
UNFIRED; NO OVERSTRAIN							
e 3	1280	89	187	345	1275	10,094	0.01
UNFIRED; OVERSTRAIN							
f 6	1020	89	187	345	758	23,152	0.01

concentration factor at the rifling radius was included in the Eq. (6) calculations of $\Delta\sigma$ by setting $k_{t\text{-}\theta} = 1.7$, so that the applied stresses were increased by this factor. No increase in the residual stresses was made, that is, $k_{t\text{-}ov} = 1.0$, based on the belief that any potential increase in the residual stress at the rifling radius would have been relieved by the machining of the rifling or by yielding at the root radius of the rifling. Expressions for the applied and residual stresses in the vessel, σ_θ and σ_{ov}, were obtained from Roark and Young (1975) and Hill (1950), respectively. The σ_r and p_{hole} terms do not apply to bore cracks so were not used.

The results in Fig. 2 are logical in some respects. The fired cannon tubes have generally lower lives than the unfired, and the overstrained cannon tubes have generally higher lives than those with no overstrain. However, the overall trend is a significant variation in fatigue life while stress range is relatively constant. This suggests that another important variable that controls fatigue life should be considered, such as the different initial crack sizes. Table 1 lists the variations in initial crack size that are known to have been present in these tubes. Unfired tubes have naturally occurring inclusions or surface roughness corresponding to about 0.01 mm deep initial cracks, whereas fired tubes typically have 0.1 mm deep heat check cracks. The group *b* fired tubes were found to have unusually deep heat check cracks of about 0.5 mm, and metallographic tests showed that one group *b* tube had an even deeper initial crack, discussed later.

The bore failure results are replotted in Fig. 3 by using the single parameter discussed earlier to account for the differences in initial crack size. The stress range has been modified to include $a_i^{(1/2 - 1/m)}$ which, for m = 3, becomes $a_i^{1/6}$. Values of a_i in meters were used to calculate $(\Delta\sigma \times a_i^{1/6})$. Note that the single parameter plotting of the results shows a somewhat more consistent trend toward an increase in life with a decrease in $\Delta\sigma \times a_i^{1/6}$. Also it is easier to see

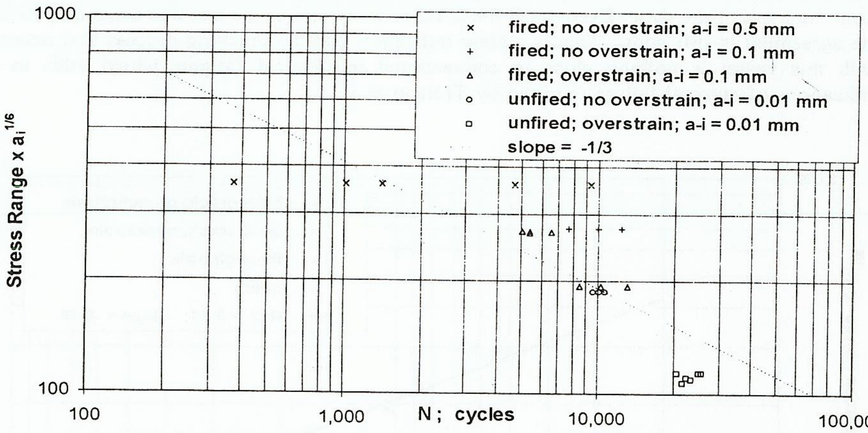

Fig. 3 - Effect of Bore Stress Range and Initial Crack Size on Life

in this plot that the fired tube results include considerably more variation than the unfired tube results. This is caused by the variation in the number and type of cannon firings performed

before the hydraulic pressure cycles. The overall trend of the results follows the arbitrary line with slope = -1/3, but with the variation noted above.

Fatigue Failure at a Stress Concentrator

Results from another group of 17 cannon pressure vessels, each with fatigue failure at a significant stress concentrator, are shown in Table 2 and Fig. 4. Various notch and through-wall hole configurations of the types shown in Fig. 1 were tested. The through-wall holes were 2 mm in diameter oriented at 30 degrees to the vessel axis to allow exit of the cannon combustion gasses. The Eq. (6) calculations for the vessels with holes included the $k_{t\text{-}\theta}$ σ_θ,

Table 2 - Vessels with Fatigue Failure at a Stress Concentrator; see Fig. 4

Type/Number of Vessels		Yield Strength *MPa*	Inner Radius *mm*	Outer Radius *mm*	Applied Pressure *MPa*	Stress Range *MPa*	Fatigue Life *cycles*	Initial Crack *mm*
THROUGH-HOLE; K_t = 3.00								
g	2	1240	53	76	207	1797	5,240	0.01
h	2	1170	60	94	297	1657	5,535	0.01
i	2	1220	78	107	83	664	42,025	0.01
EXTERNAL NOTCH; K_t = 3.26								
j	3	1230	78	142	393	1196	11,960	0.01
	1	1240	78	142	393	1196	5,501	>0.01
MID-WALL NOTCH; K_t = 2.26								
k	2	1240	85	153	406	1397	10,605	0.01
INTERNAL NOTCH; K_t = 1.26								
l	5	1070	60	135	670	1702	3,159	0.01

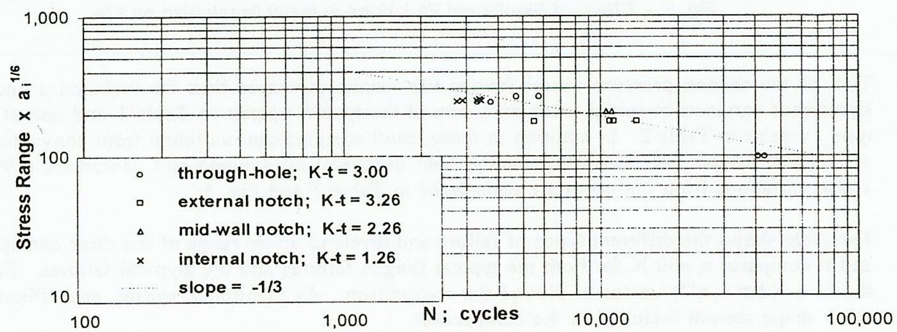

Fig. 4 - Effect of Nominal Stress Range, Stress Concentration and Initial Crack Size on Fatigue Life

p_{hole} and p_{crack} terms; the other two terms do not affect $\Delta\sigma$. The calculations for external and mid-wall notches included the $k_{t\text{-}\theta}\ \sigma_\theta$ and σ_r terms; the calculations with internal notches included all terms in Eq. (6), including effects of overstrain residual stresses. The values of k_t for the through-wall holes and the array of twenty four semicircular mid-wall notches were based on the known value of 3, with a reduction in the case of the mid-wall notches because of their close spacing. The values of k_t for the external and internal notches were from Eq. (7).

The results in Fig. 4 for failure at a stress concentrator show a similar trend to the Fig. 3 results for failure at the bore. As in Fig. 3, there is a consistent trend toward an increase in life with a decrease in $\Delta\sigma \times a_i^{1/6}$, and the results are in approximate agreement with the same line with slope = -1/3 shown earlier.

Significant Variation in Initial Crack Size

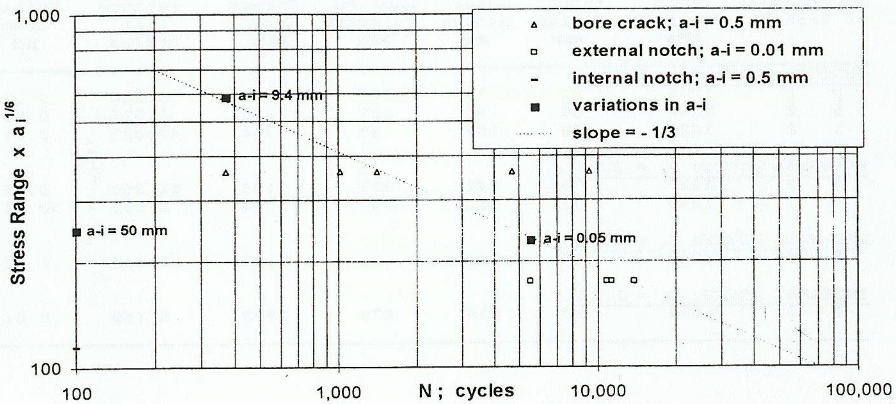

Fig. 5 - Effect of Significant Variations in Initial Crack Size on Life

Two of the cannon pressure vessel fatigue life results discussed thus far included a known significant variation in initial crack size, one of the type *b* vessels in Table 1 and one of the type *j* vessels in Table 2. In addition to these, another significant variation from conventional mechanical fatigue cracking has recently been described by Troiano and coworkers (1997). These variations from the norm are considered in Table 3 and Fig. 5.

The table shows the different types of failure and levels of stress range of the three examples, and it compares a_i and N for both the typical fatigue failures and the atypical failures. Fig 5 shows a $(\Delta\sigma \times a_i^{1/6})$ versus N plot of the comparison. As mentioned earlier, any effects of crack shape are not included in the comparison.

The bore crack test with variation in a_i showed intergranular failure on the fracture surface, typical evidence of environmental fracture. If the 9.4 mm crack present at failure had been

wholly due to environmental cracking, the result shown in the plot is in reasonable agreement with the -1/3 slope trend of the data.

Table 3 - Vessels with Significant Variations in Initial Crack Size; see Fig. 5

Type of Failure	Stress Range *MPa*	Fatigue Failure a_i *mm*	N *cycles*	Atypical Failure a_i *mm*	N *cycles*	cause
bore crack	892	0.5	4,110	9.4	373	environment
external notch	1196	0.01	11,960	0.05	5,501	machining
internal notch	405	0.5	48,000 CALCULATED	50	100	environment

The external notch test with variation in a_i also included a metallographic study that showed a 0.05 mm deep initial crack due to an aggressive machining process, compared with the expected value of 0.01 mm in unaffected material. Note in Fig. 5 that the use of the deeper crack based on metallographic results is in good agreement with the -1/3 slope trend of the data.

The last example of the effect of a significant variation in a_i on fatigue life provides the most striking results. Data from a 100 cycle life test reported by Troiano et al is plotted in Fig. 5, with $(\Delta\sigma \times a_i^{1/6})$ determined using a_i = 0.5 mm, the largest value that could be expected for normal cannon conditions. However this plotted point is nearly three orders of magnitude away from the trend of the data. Even when the a_i value at the end of the test was used, a_i = 50 mm, the agreement is still poor. This is a clear indication that the cracking process that occurred with this vessel is nothing close to conventional mechanical fatigue, which adds to the indications of atypical failure reported by Troiano et al.

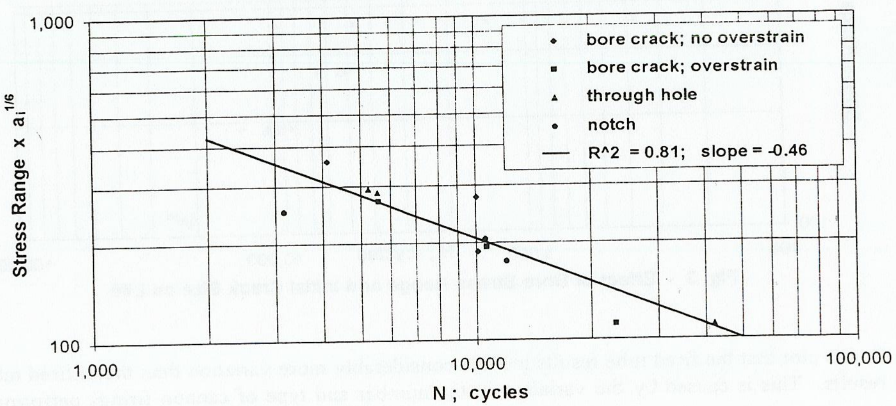

Fig. 6 - Comparison of Mean Life Results

Variation in Material Yield Strength

It may be useful to consider a summary plot of all the results discussed thus far, keeping in mind that material yield strength, an important control variable for fatigue, has not yet been addressed. Fig. 6 shows such a plot, which can be the basis for addressing yield strength effects. Twelve mean values of ($\Delta\sigma \times a_i^{1/6}$) and N are plotted, calculated from each of the twelve types of vessel data listed in Tables 1 and 2, designated *a* through *l*. The data with atypical a_i variations discussed above were not included in the mean values. Considering the inherent variations in fatigue life tests, the trend of the summary of results in Fig. 6 is quite consistent. Standard linear regression of log ($\Delta\sigma \times a_i^{1/6}$) versus log N produced the line shown, with correlation coefficient $R^2 = 0.81$ and slope = -0.46.

The summary results of Fig. 6 are presented in Fig. 7 with a modification in the single parameter to account for the effect of material yield strength. The single parameter representation of local stress range, initial crack size and material yield strength, takes the form:

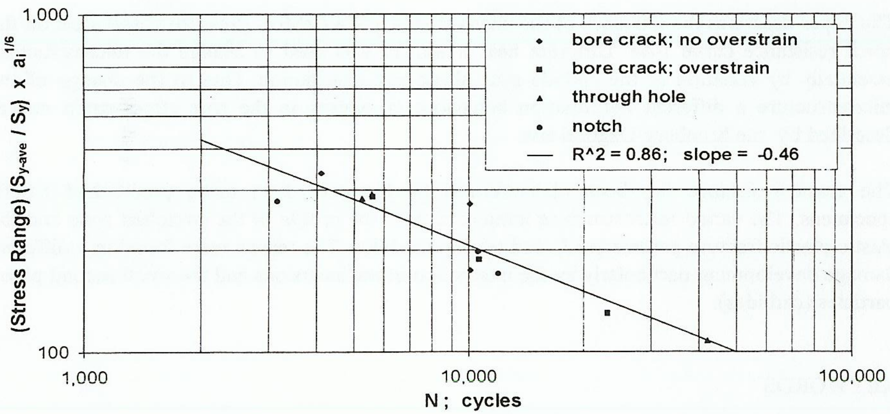

Fig. 7 - Mean Life Results Including Yield Strength Effect

$$\text{fatigue intensity factor} = \Delta\sigma \times (S_{y\text{-ave}} / S_y) \times a_i^{1/6} \qquad (8)$$

Eq. (8) is proposed as a parameter that describes the intensity of the fatigue loading of a structural component, including the important effect of material strength as well as the effects of stresses and initial crack at the failure site. The ($S_{y\text{-ave}} / S_y$) term effectively increases the stress range for a specimen with yield strength lower than the mean value, $S_{y\text{-ave}}$, and this is consistent with the shorter life expected for a decrease in strength. The ($S_{y\text{-ave}} / S_y$) form has the advantage of approaching unity when there is little difference in strength.

Note in Fig. 7 that results for materials with strength most different from the mean strength

moved closer to the regression line. This resulted in an increase in R^2 from 0.81 to 0.86, but no significant change in the position or slope of the regression line. This supports the inclusion of the material yield strength effect in the concept of fatigue intensity factor as discussed here.

Finally, using Eq. (8) it can be shown that a general form of the material strength effect in the single parameter description of fatigue life is:

$$\text{fatigue intensity factor} = \Delta\sigma \times (S_{y\text{-ave}} / S_y)^{2/m} \times a_i^{1/6} \qquad (9)$$

The $(S_{y\text{-ave}} / S_y)^{2/m}$ term can be obtained by assuming that crack growth rate varies directly with the size of the crack-tip plastic zone, so that fatigue life varies inversely with zone size, that is, $N \propto (S_y/K)^2$. This $N \propto S_y^2$ relationship, when included in the log σ versus log N form with slope -1/m, leads to the $(S_{y\text{-ave}} / S_y)^{2/m}$ term in Eq. (9). It is interesting to note that for the value of m in Fig. 7, about 2.2, Eq. (9) gives a value for the exponent of the ($S_{y\text{-ave}} / S_y$) term of 1.1. This is close to the value of unity used in Eq. (8) to account for material strength.

SUMMARY AND CONCLUSIONS

A single parameter representation of local stress range, initial crack size and material yield strength is proposed for describing the intensity of the fatigue loading of a structural component. Use of this single parameter with logarithmic plots of fatigue lifetime provides a single straight line description of fatigue life behavior over a broad range of material, configuration and loading conditions.

Expressions for calculating the local stress range at the failure site are outlined, including effects of pressure vessel and stress concentrator configuration, applied and overstrain residual stresses, and pressure applied to hole and crack surfaces.

The single parameter approach was used in a comprehensive comparison of fatigue life results from 41 full size hydraulic pressure cycling tests of cannon pressure vessels with twelve combinations of material strength, failure location, and applied and residual stresses. A log plot of mean results of the twelve data groups is well represented by a single straight line with a negative slope reasonably close to that predicted by fracture mechanics analysis.

A significant outlier from a single parameter plot of fatigue lifetime data is a useful indicator of cracking due to other than conventional mechanical fatigue. Two examples of an outlier from the trend of cannon pressure vessel data were confirmed by fractography to be caused by environmental cracking. A third outlier was related to preexisting initial cracks due to aggressive machining.

The effect of material yield strength on fatigue behavior can be simply and well represented using the single parameter approach. The R^2 correlation coefficient of a logarithmic straight line fit to the twelve sets of cannon pressure vessel results increased from 0.81 to 0.86 upon inclusion of the effect of material strength.

ACKNOWLEDGEMENTS

The authors are pleased to acknowledge M. J. Audino of the U. S. Army Armament RD&E Center for providing a comprehensive summary of cannon pressure vessel fatigue lifetime results.

Much of this work was undertaken during an attachment by one of the authors (APP) to the Army Armament RD&E Center. The attachment was arranged via the European Research Office of the U. S. Army Research, Development and Standardization Group (UK).

REFERENCES

Audino, M. J. (1993) Fatigue Life Assessment of 155 mm M284 Cannon Tubes. Army Armament Research, Development and Engineering Center, Watervliet, NY.

Davidson, T. E., Throop, J. F. and Underwood, J. H. (1977). In: *Case Studies in Fracture Mechanics*, (T. P. Rich and D. J. Cartwright, eds.). pp. 3.9.1 - 3.9.13. Army Materials and Mechanics Research Center, Watertown, MA.

Hill, R. (1950). *The Mathematical Theory of Plasticity*, Clarendon Press, Oxford.

Maddox, S. J. (1971). "Fracture Mechanics Applied to Fatigue in Welded Structures," In: *Welding Institute Conference on Fatigue of Welded Structures*, The Welding Institute, Cambridge, 73-96.

Paris, P. C. and Erdogan, F. (1963). *J. of Basic Engineering*, 85, 528-534.

Parker, A. P., Endersby, S. N., Bond, T. J., Underwood, J. H., Lee, S. L. and Higgins, J. (1996). In: Proceedings of PVP Conference (July 1996) , ASME, New York, in press.

Parker, A. P. and Underwood, J. H. (1997). In: *Fatigue and Fracture Mechanics: Twenty Eighth Volume, STP 1321*, ASTM, Philadelphia, in press.

Roark, R. J. and Young, W. C. (1975). *Formulas for Stress and Strain*, McGraw-Hill, New York.

Troiano, E., Underwood, J. H., Scalise, A., O'Hara, G. P. and Crayon, D. (1997). In: *Fatigue and Fracture Mechanics: Twenty Eighth Volume, STP 1321*, ASTM, Philadelphia, in press.

Underwood, J. H. and Parker, A. P. (1995) *J. of Pressure Vessel Technology*, 117, 222-226.

Underwood, J. H., Parker, A. P., Corrigan, D. J. and Audino, M. J. (1995) In: *PVP - Vol. 316, Plant Systems/Components Aging Management*, ASME, New York, 154-161.